Spray-induced gene silencing targeting a glutathione S-transferase gene improves resilience to drought in grapevine

Chiara Pagliarani ORCID iD: 0000-0003-4656-6192

Mirko De Rosso ORCID iD: 0000-0003-4005-7012

WALTER CHITARRA ORCID iD: 0000-0002-5382-3794

Spray induced gene silencing targeting a glutathione S-transferase gene improves resilience to drought in grapevine

Running head: SIGS to induce drought resilience in grapevine

Luca Nerva[a,b,*], Micol Guaschino[a,c], Chiara Pagliarani[b*], Mirko De Rosso[a], Claudio Lovisolo[c], Walter Chitarra[a,b,*]

[a]Council for Agricultural Research and Economics - Research Centre for Viticulture and Enology (CREA-VE). Via XXVIII Aprile, 26; 31015 Conegliano (TV), Italy

[b]National Research Council of Italy - Institute for Sustainable Plant Protection (IPSP-CNR). Strada delle Cacce, 73; 10135 Torino (TO), Italy

[c]Department of Agricultural, Forest and Food Sciences (DISAFA), University of Torino, Largo Paolo Braccini 2, 10095 Grugliasco (TO), Italy

Corresponding authors details

Walter Chitarra – walter.chitarra@crea.gov.it

CREA - Research Centre for Viticulture and Enology (CREA-VE)

Via XXVIII Aprile, 26

31015 Conegliano (TV), Italy

Luca Nerva – luca.nerva@crea.gov.it

CREA - Research Centre for Viticulture and Enology (CREA-VE)

Via XXVIII Aprile, 26

This article has been accepted for publication and undergone full peer review but has not been through the copyediting, typesetting, pagination and proofreading process, which may lead to differences between this version and the Version of Record. Please cite this article as doi: 10.1111/pce.14228.

31015 Conegliano (TV), Italy

Chiara Pagliarani – chiara.pagliarani@ipsp.cnr.it

CNR - Institute for Sustainable Plant Protection (IPSP-CNR)

Strada delle Cacce, 73

10135 Torino (TO), Italy

Keywords

dsRNAs, RNA interference, gas exchange, abscisic acid, abiotic stress, stilbenes, foliar application, *Vitis vinifera*

Abstract

Along with the ongoing climate change, drought events are predicted to become more severe. In this context, the Spray Induced Gene Silencing (SIGS) technique could represent a useful strategy to improve crop stress resilience. A previous study demonstrated that the Arabidopsis mutants for a glutathione S-transferase (*GST*) gene had increased abscisic acid (ABA) levels and a more activated anti-oxidant system, both features that improved drought resilience.

Here, we used SIGS to target a putative grape *GST* gene (*VvGST40*). Then, ecophysiological, biochemical and molecular responses of 'Chardonnay' cuttings were analysed during a drought and recovery time-course. Gas exchange, ABA and *t*-resveratrol concentration as well as expression of stress-related genes were monitored in not treated controls, dsRNA-*VvGST40*- and dsRNA-*GFP*- (negative control of the technique) treated plants, either submitted or not to drought.

VvGST40-treated plants revealed increased resilience to severe drought as attested by the ecophysiological data. Analysis of target metabolites and antioxidant- and ABA-related transcripts confirmed that *VvGST40*-treated plants were in a priming status compared with controls.SIGS targeting an endogenous gene was successfully applied in grapevine, confirming the ability of this technique to be exploited not only for plant protection issues but also for functional genomic studies.

Summary statement

Here, we used the innovative SIGS technique to functionally characterize a glutathione-S-transferase (*VvGST40*) gene in grapevine which indeed showed an improved resilience when submitted to severe water stress treatment.

1. Introduction

Climate future projections give a collective picture of a substantial drying and warming of the Mediterranean region, exposing crops to increasingly frequent drought events. Adaptation of agriculture to climate change relies on a complex network of biological mechanisms, especially for those perennial species that can produce for decades (Lionello *et al.*, 2006).

Today, it is increasingly impellent to find new sustainable systems able to cope stressful conditions (*e.g.* drought) and preserve the limited resources using, for example, New Plant Breeding Techniques or RNA interference technologies (Giudice *et al.*, 2021). The latter technology relies on the RNA interference (RNAi) process, naturally occurring in eukaryotic cells, to regulate gene expression in response to the presence of double stranded RNAs (dsRNAs) (Hannon, 2002). In plant cells, the RNAi pathway is triggered by dsRNAs that are recognized and converted into fragments of 20-24 nt long RNA duplexes (short interfering RNAs, siRNAs) by DICER-LIKE endonucleases (Kusaba, 2004). These siRNAs are then loaded into ARGONAUTE proteins forming the RNA-induced silencing complexes (RISCs) thus leading to post-transcriptional gene silencing (PTGS) (Kim, 2008). In nature, RNAi mediates resistance to pathogen attacks involving the introduction of foreign nucleic acids (*e.g.* viral infections). It is also a process that regulates expression of endogenous protein encoding genes through the production of microRNAs (miRNAs) (Reinhart *et al.*, 2002). Only recently, artificial introduction of exogenous dsRNAs or small RNAs (sRNAs) in plant tissues has been adopted as an alternative tool for disease management against pathogen or insect attacks and, although to a lesser extent, to regulate plant gene expression in a sequence-specific manner (Dalakouras *et al.*, 2020; Nerva *et al.*, 2020). Only a few studies and one patent dealing with the down-regulation of plant genes after exogenous application of dsRNA molecules are currently available in literature (Lau *et al.*, 2015; Li *et al.*, 2015; Warnock *et al.*, 2016; Kiselev *et al.*, 2021a,b; Marcianò *et al.*, 2021). RDR6-mediated systemic

silencing leads to transient amplification of siRNAs in plant tissues once the concentration of 22-nt siRNAs exceeds a threshold value able to trigger this pathway (Kalantidis *et al.*, 2008). Transitivity processes are yet unclear, however recent evidence suggested that intronless genes are mostly subjected to RDR6 activity, thus more frequently undergoing transitivity and systemic silencing phenomena in respect to intron-containing genes, for which the onset of RNAi commonly occurs locally in the treated tissues (Dalakouras *et al.*, 2020). One of the most recent application methods of exogenous dsRNAs in plants is the so-called Spray Induced Gene Silencing (SIGS). This technique consists in high or low pressure spraying of dsRNAs on plant leaves to activate the plant RNAi machinery leading to siRNA accumulation. Foliar dsRNA application is affected by different variables that can influence dsRNA effectiveness and persistence in planta (*e.g.* environmental conditions, UV, microbe-derived degradation, etc.). To date, several strategies for improving dsRNA delivery and stability are under scrutiny. For example, surfactants or nanotechnology-based delivery systems have been used to successfully maintain the stability of the applied nucleic acids (*e.g.* Numata *et al.*, 2014; Mitter *et al.*, 2017). In this line, recent studies defined the best conditions (*e.g.* plant age, timing of application, soil moisture) to efficiently apply dsRNAs on leaf surfaces (Kiselev *et al.*, 2021b,a).

Drought is one of the major abiotic stressful factors affecting agriculture. Water plays a crucial role in plant growth, development, metabolism and biochemistry, being the most important resource, and contemporarily the most limiting one. Drought impairs plant metabolism and productivity by altering the physiological status and triggering dynamic responses to alleviate its negative effects. Grapevine cultivation in the Mediterranean area does not generally involve the use of irrigation, being this traditionally considered a rainfed crop (Lovisolo *et al.*, 2016). Grapevine has been used as a model woody plant to study ecophysiological responses to water stress since the seventies (Lovisolo *et al.*, 2010; Belfiore *et al.*, 2021). Furthermore, in recent years transcriptomic and functional genomics studies, supported by the availability of a reliable sequenced genome, allowed researchers to achieve a better understanding of grapevine molecular and physiological responses to drought. Among the plant responses mounted by plants to cope with drought, the modulation of several molecular pathways, hormonal imbalance (e.g. ABA and strigolactones), antioxidant machinery and reactive oxygen species (ROS)

scavenging mechanisms were reported (Mishra *et al.*, 2017; Belfiore *et al.*, 2021; Seleiman *et al.*, 2021).

Upon drought conditions the impairment of photosynthetic activity leads to the leakage of electrons and oxygen, that can eventually act as electron acceptors, in turn generating the superoxide radical O_2^- in chloroplasts (Fischer *et al.*, 2013). Further pathways can lead to O_2 reduction to hydrogen peroxide (H_2O_2), which is considered a signaling molecule in presence of different types of abiotic stresses, specifically in grapevine (Ferrandino & Lovisolo, 2014). ROS are able to react with proteins, cellular components, lipids and nucleic acids, leading to oxidative damage if not properly scavenged either through enzymes like catalases, peroxidases, dismutases or through non-enzymatic antioxidants like glutathione (GSH) and ascorbate (Asc) (Wang *et al.*, 2019). GSH in plants, besides a role in preventing oxidation damage, also functions as a substrate for glutathione-S-transferases (GST), which belong to a large heterogeneous family of proteins divided in fourteen different classes (Labudda & Safiul Azam, 2014). Plant GSTs, due to their catalytic domain conformation, hold certain heterogeneity of functions and ligand promiscuity. For these reasons, different biotechnological approaches are reported in literature aiming to study the modulation of GSTs and their potentiality in abiotic stress resilience. Despite the widely assumed involvement of GSH in stress signaling in plants, to the best of our knowledge only one example of drought and salt stress tolerance mediated by GSH have been reported up to date. Remarkably, Chen *et al.* (2012) demonstrated that the knock-out of *AtGSTU17* increased drought and salt stress tolerance in Arabidopsis as a result of the combined GSH and ABA positive effects linked to overaccumulation of these two molecules in knock-out mutants. More in detail, GSTs are involved in the detoxification of xenobiotics and/or the conjugation with other substrates for signaling transduction pathways using GSH (Foyer & Noctor, 2005, 2009). The knock-out *atgstu17* mutants are unable to exploit the GSH pool for these cellular processes, leading to a significant intracellular overaccumulation of GSH (Chen *et al.*, 2012). As previously stated, GSH works as an important cellular signaling compound that influences many fundamental cellular processes in turn impacting on many physiological responses. During drought, an increased burst of reactive oxygen species, as a consequence of oxidative stress, is observed, and hence the overaccumulation of GSH in *atgstu17* plants is the probable cause of the observed tolerant phenotype (Chen *et al.*, 2012).

Based on the above, we addressed our study to test the effectiveness of SIGS as a rapid and reliable tool to improve drought stress resilience in a woody plant species typically recalcitrant to traditional functional genomics approaches (Giudice *et al.*, 2021). In particular, we outlined the effects of SIGS by means of high-pressure foliar application of dsRNAs targeting the grape homologue of *AtGSTU17* (named as *VvGST40*), in rooted cuttings of *Vitis vinifera* cv Chardonnay subjected to drought. To this aim, leaves were treated prior to stress imposition, then responses of plants were monitored during drought and recovery time-courses by using molecular, biochemical and ecophysiological approaches.

2. Materials and Methods

2.1 Gene identification and cloning

The GST sequence used in this study was the homologue of the Arabidopsis functional *GST* characterized by Chen *et al.* (2012). The sequence of the closest corresponding protein in *V.vinifera* resulted to be VIT_01s0026g01340 which was selected by performing a BLAST nucleotide research against the Chardonnay genome available at http://169.237.73.197/Chardonnay04/ (Zhou *et al.*, 2019). The first step was the primer design for the putative *Vitis GST* gene (following referred to as *VvGST40*) to obtain an amplification product around the size of 700bp (Fig. 1a). The sequence of the amplicon has been used to perform a target specificity analysis using the si-Fi software (Lück *et al.*, 2019) and to avoid possible off-target effects on other genes. Primer pairs were designed using the online tool Primer3 (https://primer3.ut.ee/), on the non-conserved region of the gene (For: 5'-AACTCGGTTGCTCTGCTTGA-3'; Rev: 5'-ACCCCAAGAAGCAACCCAAA-3'). The obtained intron-less amplicon was then cloned within the expression vector L4440 by performing an enzymatic digestion with the restriction enzyme PstI following the manufacturer's instruction (Thermo Fisher Scientific, MA, USA).

2.2 dsRNAs synthesis and application method

dsRNAs were synthetized *in vitro* as previously reported by Ahn et al. (2019), the protocol includes a transformation step of the cloned fragments in dH5α *E.coli* cells to produce large amounts of plasmid prior to RNA production following the manufacturer's

instruction of the MAXIscript™ T7 Transcription Kit (Thermo Fisher Scientific, MA, USA). In detail, two different types of dsRNAs were produced: one targeting *GFP* (Nerva *et al.*, 2020) and one targeting the putative *VvGST40* gene (Supplementary Fig. 1).

Application of the synthetized dsRNAs was performed through SIGS approach (Nerva *et al.*, 2020) using the high pressure (10 bar) spraying technique with an airbrush on the abaxial side of the leaves. The dsRNA application was performed twice for both *VvGST40* and *GFP* genes (used as negative control of the technique): 7 and 4 days before the drought stress imposition, using 50 µg (Dubrovina *et al.*, 2019; Nerva *et al.*, 2020) per plant in each treatment (Supplementary Fig. 2).

2.3 Plant material and experimental design

One-year-old potted *Vitis vinifera* cv Chardonnay woody cuttings were kept in open air conditions at the experimental station of CREA-VE (45.852782N,12.255926E). The chosen substrate was a not sterilized mixture of vineyard soil/sphagnum peat (8:2, v:v) to better simulate the field conditions. The substrate composition was a sandy-loam soil (pH 7.8; available P 10.4 mg kg^{-1}, organic matter 6,07%; cation exchange capacity 20.11 mew 100 g^{-1}).

The experimental setup consisted of two conditions (well-watered (NS) and water stress (WS)) for each of the three treatments: i) dsRNAs targeting the *VvGST40*; ii) dsRNAs targeting the *GFP* and iii) not treated control treatments (CTRL) (four plants for each treatment and condition, 24 plants in total). Once treated and the stress imposed, each plant was monitored by means of leaf gas exchange for the whole duration of the time course (18 days; Supplementary Fig. 2). When net photosynthesis or stomatal conductance was around zero (defining the severe WS point as reported by Lovisolo *et al.*, 2010 and Belfiore *et al.*, 2021), WS plants were rehydrated and recovery was monitored. For each treatment and condition, leaf samples were collected prior to stress imposition, at the severe stress point and at full recovery (*i.e.* T0, T2, T4, T6 for all treatments and T18 for *VvGST40* plants only) (Supplementary Fig. 2). Weather conditions were monitored over time using the CREA-VE weather station coupled to a Watch Dog 1400 datalogger instrumentation (Spectrum Technologies, Bridgend, UK) (Supplementary Fig. 3). At each sampling point, three biological replicates were

collected for molecular and target metabolite analysis: each biological replicate was formed by pooling one leaf from each plant from the same condition and treatment (*i.e.* 4 leaves in total). Thus, samples were immediately frozen in liquid nitrogen and stored at -80 °C until use.

2.4 Leaf gas exchange measurements

Net photosynthesis (Pn), stomatal conductance (g_s) and intercellular CO_2 concentration (Ci) were measured on all plants between 10:00 and 13:00 h on each experimental day. For each plant, one fully developed non-senescing leaf growing between the 5th and the 8th shoot from the base was measured at ambient photosynthetic photon flux density (PPFD) using a Ciras 2 portable system (PP SYSTEMS Europe, Herts, UK).

2.5 RNA isolation and gene expression analysis

Collected samples were processed to isolate total RNA starting from 50 mg of lyophilized leaves and using the Spectrum™ Plant Total RNA Kit (Sigma-Aldrich, USA), following manufacturer's instructions except for the substitution of 2-mercaptoethanol with sodium metabisulfite for RNA preservation. RNA concentration of the extracted samples was quantified at the NanoDrop™ (Thermo Fisher Scientific, MA, USA), RNA quality was further checked at the Bioanalyzer (2100 Bioanalyzer, Agilent Technologies), and only samples showing RIN (RNA integrity number) > 8 were used for real-time PCR analyses. RNA samples were treated with DNase I (Thermo Fisher Scientific, MA, USA) following manufacturer's instruction. The absence of genomic DNA was checked before cDNA synthesis by quantitative real time PCR (qPCR) using *VvCOX* specific primer of grapevine (Supplementary table 1). After DNase treatment, samples were subjected to cDNA synthesis using the High-Capacity cDNA Reverse Transcription Kit (Applied Biosystems, Thermo Fisher Scientific, MA, USA) starting from 1 µg of total RNA.

qPCR reactions were carried out in a final volume of 10 µL using the SYBR® Green protocol (Bio-Rad Laboratories Inc., USA) and 1:5 diluted cDNA as template (Chitarra *et al.*, 2018). Reactions were run in a Bio-Rad CFX96 instrument (Bio-Rad Laboratories Inc., USA) using the following conditions: an initial denaturation phase at 95°C for 3 min, followed by 40 cycles at 95°C for 10 s and 60°C for 30 s. Each amplification was followed by melting curve analysis (65-95°C) with a heating rate of 0.5°C every 5 s. All

reactions were performed with at least two technical replicates. Relative expression level was carried out using a comparative threshold cycle approach ($\Delta\Delta C_t$ method), normalizing the expression to the housekeeping genes cytochrome-C-oxidase (*VvCOX*) and actin (*VvACT*). Gene expression data were calculated as expression ratio (Relative Quantity) to CTRL NS at T0. Oligonucleotide sequences are listed in Supplementary Table 1. The primer pair for *VvGST40* was designed outside from the region targeted by the dsRNAs in order to avoid over-quantification of the endogenous transcripts.

2.6 Analysis of target metabolites

About 100 mg of the lyophilized leaves used for total RNA isolation were processed for the HPLC-DAD analysis. Briefly, the extraction buffer was aliquoted in each sample: 750 µL of 80% methanol-H_2O (8:2 v/v) with 0,1% of acetic acid. The mixture was then subjected to sonication in an ultrasonic bath for 1h at maximum intensity. After the sonication step, samples were centrifuged at maximum speed for 10' at 4°C. Before quantification, the samples were filtrated using a 0.20 µm PTFE membrane filter (Chromafil® Xtra PTFE-20/13, Macherey-Nagel, Germany).

A Thermo Finnigan Spectra SYSTEM instrument (Thermo Finnigan, San Jose, CA) equipped with AS3000 autosampler, column temperature controller, diode array detector (DAD, UV6000LP), P4000 quaternary pump and SCM1000 online degasser was adopted for HPLC analyses. A C_{18} column (4.6 mm × 150 mm, 5 µm, XTerra®RP18) was used for the chromatographic separations. The analytical method and the flow rate were maintained as previously reported (Irankhah *et al.*, 2020a; Pagliarani *et al.*, 2020; Belfiore *et al.*, 2021). Briefly, the analysis was carried out in reverse phase with an elution gradient method. Eluent A was 0.1% formic acid in water and eluent B was acetonitrile; flow rate was fixed at 500 µL min^{-1}: from 10% to 35% of B in 20 min, from 35% to 100% of B in 5 min, 100% of B for 5 min, from 100% to 10% in 1 min, conditioning for 10 min. Twenty microliters were injected for each sample and three biological replicates were run for each analysis. Detection wavelengths were set at 265 nm (ABA) and 307 nm (*t*-resveratrol). Original standards of *t*-resveratrol (purity ≥ 99%) and abscisic acid (ABA, purity ≥ 98.5%) purchased from Merck KGaA (Darmstad, Germany) were used to prepare the calibration curves.

2.7 Data analysis

Data were analyzed by one-way analysis of variance (ANOVA) using time as the main factor. Analysis was performed by SPSS statistical software package v. 23.0 (SPSS Inc., Cary, NC, USA). The Tukey's HSD post hoc test was used when ANOVA showed significant differences at a probability level of $P \leq 0.05$.

3. Results

3.1 Target gene silencing and evaluation of exogenous dsRNA persistence on leaves

We first addressed our survey to assess the effectiveness of the SIGS technique in silencing target endogenous plant genes. *VvGST40* was the gene chosen for the application of the SIGS technology in this study, and its relative expression level was analyzed during the whole experimental time course for each treatment and condition (Fig. 1).

In CTRL WS, the *VvGST40* expression almost halved from T0 to T2 when the severe stress took place (see below, Fig. 1b). *GFP* WS showed a similar trend, attesting a down-regulation of this gene upon water stress conditions. On the contrary, in *VvGST40* plants, the treatment induced a silencing effect even when the vines were not subjected to water limitation. In fact, in these plants at T0, *VvGST40* showed a significantly lower expression both in NS and WS conditions in comparison with the other treatments. Furthermore, *VvGST40* WS vines took two days more than the others to reach the same level of severe stress (T4, see below). Concomitantly, at T4 the *VvGST40* expression dropped below 0.4 in these plants, reaching the lowest expression level among all samples and treatments. Only at T2 the *VvGST40* expression trend was not clearly different among the samples, likely due to unknown environmental conditions that influenced the plant performances (Fig. 1b).

It is worth noting that, in this study, a specific and off-target free sequence of *VvGST40* has been selected, but other similar approaches on large gene families could lead to down-regulation of off-targets with unpredictable physiological, molecular, and phenotypic responses. For this reason, the selection of a target-specific sequence as well as the *in-silico* prediction of potential off-targets (Lück *et al.*, 2019) have to be addressed prior to SIGS application.

Finally, a qPCR analysis was performed on *GFP*-treated plants to evaluate the persistence of the exogenous dsRNAs on the leaf surface. Since the objective here was to determine how long the dsRNA molecules could persist within the plant, this experiment did not include any nuclease treatment to distinguish between the GFP dsRNAs present on the leaf surface from those potentially unloaded into the mesophyll. However, the collected results indicated that *GFP* was still detectable in leaves until 10 days after the last SIGS application (ie. T6; Fig. 1c).

3.2 Analysis of leaf ecophysiology reveals resilience to drought in *VvGST40*-primed plants

Leaf gas exchanges were daily monitored from the water stress imposition day (T0) till the end of the experiment (T18) (Figs. 2 and S2). G_s and Pn trends were followed to define the severe stress point for each treatment (ranging around zero for both parameters). It is worth noting that, although not significant, at T0 *VvGST40*-primed plants displayed lower g_s values than CTRL and *GFP* ones, suggesting a certain degree of stomata limitation already in NS conditions (Fig. 2a). This was likely due to the increased levels of endogenous ABA, which were significantly higher in *VvGST40*-primed plants than others (see ABA results, Fig. 3a). Conversely, independently of stress imposition, g_s rates were similar both in *GFP* and CTRL plants. In detail, CTRL and *GFP* plants experienced a dramatic drop in g_s values already two days after WS imposition (at T2), reaching a complete stomatal closure. After re-watering, both CTRL and *GFP* vines fully recovered g_s rates within four days (Fig. 2a). The physiological response to drought and recovery was different in *VvGST40* plants, which not only showed a delay in stomatal closure (reached at T4) during the water stress time course, but they also had significantly slower recovery dynamics (ie. fourteen days were needed to complete recovery, as attested by both g_s and Pn measurements) with respect to CTRL WS and *GFP* WS plants (Fig. 2a,b).

Based on the threshold defined to establish a photosynthesis regulation model, regardless of the cultivar (Flexas *et al.*, 2002; Medrano *et al.*, 2002), stomatal closure is strictly linked to photosynthesis (Pn). Accordingly, Pn measurements well correlated here with the delay in stomatal closure (Fig. 2b), as the trend of Pn values in *VvGST40* WS plants resembled that observed for g_s. More in detail, *VvGST40* WS plants delayed the photosynthetic failure (up to T4) and did not reach assimilation values as lower as those

recorded for CTRL WS and *GFP* WS plants at T2. Furthermore, as observed for the g_s recovery trend, *VvGST40* WS plants recovered Pn more slowly than CTRL NS and *GFP* NS grapevines (ie. fourteen days after re-watering, T18, Fig. 2b). Conversely, in NS plants the Pn trend was similar among treatments.

Ci rates were also monitored in all plants over the treatment duration, and as expected they were found significantly higher at the severe WS point than in NS condition for both CTRL and *GFP* plants (T2) and for *VvGST40* plants (T4), in which they remained high till the day of full recovery at T18 (Fig. 2c). This trend further confirmed the photosynthetic inhibition induced by drought stress that leads to the accumulation of intercellular CO_2 into the substomatal chamber, as a consequence of the metabolic-mediated stomatal limitation (Belfiore *et al.*, 2021).

3.3 ABA metabolism and related signaling pathways are enhanced in *VvGST40*-primed plants under drought

In search for evidence supporting the peculiar physiological dynamics observed in *VvGST40*-primed plants, we quantified ABA concentrations in leaves taken from all experimental conditions over the whole time-course duration. At T0 leaf ABA level was significantly higher only in *VvGST40* samples (Fig. 3a), while at T2 it increased in all the analyzed WS samples, although the hormone quantity was slightly higher following SIGS application in comparison with CTRL and *GFP* WS samples (Fig. 3a). This finding could support the lower values recorded for Pn and g_s in *VvGST40*-primed plants prior to stress imposition and also at T2 with respect to T0 (Figs. 2 and 3a). During the time-course, ABA concentration progressively raised in *VvGST40*-primed plants showing a peak of accumulation at the moment of maximum stress (T4). After the re-watering treatment, no significant differences were observed in ABA levels when NS and WS samples were compared, including the *VvGST40* ones. This result was most likely due to the transient silencing of the endogenous gene induced by SIGS application (Dalakouras *et al.*, 2020).

Additionally, to gain a more comprehensive overview of the specific biochemical responses of *VvGST40*-primed plants, the expression profiles of key genes involved in ABA biosynthesis and degradation were analyzed in the same samples.

The expression of the ABA biosynthetic gene *VvNCED3* was significantly higher at T2 in all WS samples compared with the related NS controls (Fig. 3b), following what observed for ABA accumulation patterns. In *VvGST40* WS plants the transcriptional profiles of *VvNCED3* started to increase at T2 and then underwent a sharp up-regulation (up to 30-fold than controls) at T4 (Fig. 3b). Unlike *NCED3*, the expression of *VvBG1*, a β-glucosidase-encoding gene that hydrolyses ABA-glucose ester in grapevine (Sun *et al.*, 2015), was significantly higher only when *VvGST40* plants perceived the maximum stress (T4; Fig. 3c), confirming the urgency to convert ABA in the active form under severe drought.

Looking at genes involved in ABA degradation pathways, the ABA-UDPG glycosyl transferase-encoding gene (*VvGT1*; Sun *et al*., 2015) was downregulated in all treatments without showing significant differences (Fig. 3d). Conversely, *VvHYD1*, homologue to an ABA 8'-hydroxylase that in Arabidopsis is typically induced by drought (Kushiro *et al.*, 2004), had an almost stable expression among the treatments, displaying a slightly higher peak at T2 in both CTRL WS and *GFP* WS plants compared with NS controls (Fig. 3e). Interestingly, at T4 *VvHYD1* was significantly up regulated already in *VvGST40* NS samples, further suggesting that the higher basal content of ABA in *VvGST40* samples encountered a different fate in homeostasis regulation under WS or NS conditions (Fig. 3e).

To strengthen these findings, we also analyzed the main genes involved in ABA sensing (i.e. *VvabaR* and *VvPP2C4*) and signaling (i.e. *VvABF1*). *VvabaR* encodes a PYR-related-8 (PYL8) protein of *Vitis vinifera*, which is widely considered as an ABA receptor. PYL8 is part of a wider protein family commonly referred to as PYR/PYL/RCAR, which is responsible for ABA binding and interaction with 2C protein phosphatases (PP2C) (Sah *et al.*, 2016). *VvabaR* transcripts were up-regulated only in *VvGST40* WS samples at T2, showing a peak of expression at T4 (Fig. 3f). Similarly, *VvPP2C4* expression was significantly higher in all WS samples at T2 and reached the maximum expression level in *VvGST40* WS plants at T4 compared with the related NS controls (Fig. 3g). The activation of the ABA responsive factor ABF is consequent to ABA signal perception by PYR/PYL/RCAR and PP2C4 proteins (Sah *et al.*, 2016). Accordingly, *VvABF1* transcripts were significantly up regulated at T2 in all WS samples, particularly in the *VvGST40* WS ones (Fig. 3h). During recovery, independently

of SIGS application, the *VvABF1* expression profiles did not significantly change between WS and NS plants (Fig. 3h). These findings further confirmed the effectiveness of the SIGS treatment-mediated priming effect, attesting that during drought stress *VvGST40* plants perceive the ABA signal before reaching severe water deficit limitations (T4).

Finally, based on the notion that strigolactone (SL) synthesis and signaling can regulate stomatal closure (Tardieu, 2016; Visentin *et al*., 2016; Visentin *et al*., 2020) and that this effect could depend, at least in part, on the cross-talk with ABA metabolic and signaling pathway (Van Ha *et al*., 2014), we quantified the transcriptional profiles of the SL biosynthetic genes *VvCCD7* and *VvCCD8*. Interestingly, in our study both *VvCCD7* and *VvCCD8* were significantly up-regulated in all WS samples at the severe stress points (T2 and T4), with higher levels in *VvGST40* WS (at T4) than related NS controls (Fig. 4a,b). Such expression patterns mirrored those observed for *VvNCED3* transcription and ABA accumulation, thereby providing further evidence for the delay in stomatal closure and photosynthesis inhibition observed in *VvGST40* plants.

3.4 Analysis of Ascorbate-Glutathione cycle (Asc-GSH)-related genes and patterns of resveratrol accumulation

The main target genes involved in Asc-GSH cycle were also analyzed to look for differences among treatments in stress perception and efficiency of ROS detoxification (Fig. 5).

At T2, transcripts of ascorbate peroxide (*VvAPX*) showed a significant increase, of about 1.5 folds, in all WS samples with respect to NS controls (Fig. 5a). Interestingly, in *VvGST40* WS leaves the *VvAPX* upregulation preceded the severe stress point (T4), suggesting an early activation of the detoxification pathway (Fig. 5a). Another key enzyme responsible for regulating stress signaling and the GSH:GSSG ratio is the glutathione reductase (GR). Notably, *VvGR* expression peaked at T2 in *GFP* WS and at T4 in *VvGST40* WS plants, in concomitance with the respective severe stress points (Fig. 5b). Additionally, during the experimental time course, dehydroascorbate reductase (*VvDHAR*) and monodehydroascorbate reductase (*VvMDHAR*) displayed a higher transcriptional activation in *GFP* WS rather than *VvGST40* WS samples (Fig. 5c,d).

To go deeply into the understanding of this varied landscape of biochemical signals, we also analyzed the accumulation patterns of *t*-resveratrol.

As expected, *t*-resveratrol concentration was significantly higher in both *GFP* and *VvGST40* leaves with respect to the related CTRLs at T0. Particularly, in the case of *GFP* samples, the metabolite levels were already high at T2, likely due to the induction of pattern-triggered immunity (PTI) responses due to the dsRNA application. At T4, *t*-resveratrol strongly increased in *VvGST40* WS plants, reaching values of about 7 µg g^{-1} DM that highlighted a SIGS mediated-priming effect particularly marked upon severe drought. This data was further corroborated by the analysis of the stilbene synthase 1 (*VvSTS1*) gene, whose expression profiles resembled the metabolite accumulation (Fig. 6a,b).

4. Discussion

4.1 SIGS is a successful strategy for silencing endogenous genes in grapevine

The first objective of this study was to assess the application of SIGS technology as a reliable and time-saving approach for performing functional genomics study in grapevine, a woody species typically recalcitrant to traditional transformation protocols (Gambino & Gribaudo, 2012). Therefore, we tested the effectiveness of the SIGS technique in silencing the endogenous grapevine gene *VvGST40*, which is the homologue of the Arabidopsis *AtGSTU17* commonly reported as repressed upon drought conditions in several plants, including grapevine (Perrone et al., 2012; Corso et al., 2015). Accordingly, we showed that severe water limitation negatively affected the expression of the target gene in absence of SIGS treatment. Interestingly, in SIGS-treated plants *VvGST40* was already down-regulated under well-watered conditions, and this transcriptional repression steadily increased with the progression of drought spell. These data could thus suggest a synergy between the effect of drought and SIGS application that prompted us to investigate more in depth the physiological and molecular responses of these plants to stress occurrence.

In parallel, we proved that, despite they were applied free of delivery vectors, dsRNAs were still present on treated leaves 10 days post foliar application, indicating a longer persistence of these molecules in the environment than previous reports. This is an

important outcome as research studies describing the endurance of exogenous-applied naked dsRNAs on leaves are still limited and only some minor information is available about the different timing of their persistence on the plant tissue surface (Giudice *et al.*, 2021). Mitter *et al.* (2017a and 2017b) showed that the northern blot analysis was able to reveal the presence of naked dsRNAs (applied through spraying) up to 5 days post-application on *Nicotiana tabacum* leaves. The authors attributed the shortness of the protective effects to the dsRNA degradation in leaves, which was estimated to occur within 5-7 days after their application. Similarly, Dubrovina *et al.* (2019) reported that transgene-encoding dsRNAs targeting the *nptII* and *EGFP* genes were stable and detectable in Arabidopsis leaves for at least 7 days post foliar application through soft brushes. The reasons that allowed us to detect dsRNAs for a longer timespan than other studies could rely on the fact that we applied the dsRNAs on the abaxial leaf surface, thus probably providing a more protected environment for them (eg. reduced exposition to UV radiation and washout effects). Remarkably, it was recently reported that dsRNAs sprayed on *A. thaliana* leaves are able to enter and spread into leaf tissues and cells, although the uptake mechanisms remain still unknown (Kiselev *et al.*, 2021b).

4.2 A boost in ABA metabolism and signaling underlies the improved resilience of *VvGST40*-primed plants to drought

The analysis of leaf gas exchanges attested that the adopted SIGS treatment targeting the *VvGST40* gene did not apparently influence the plant physiological performances under irrigation, but it rather exerted its priming effect when the treated vines experienced drought stress. Indeed, in comparison with untreated WS plants, the *VvGST40* WS vines perceived the stress later and also needed more time to recover gas exchange rates to the pre-stress levels. We therefore reasoned that the SIGS-induced downregulation of *VvGST40*, observed in these plants already upon irrigation, could have triggered molecular and biochemical signals pivotal for the establishment of stress resilience mechanisms. Indeed, as described in Arabidopsis by Chen *et al.* (2012), the delayed stomatal closure observed in *VvGST40* WS plants could rely on a SIGS-mediated priming effect most likely influencing the regulation of the stress-responsive signaling cascades involving ABA and antioxidant cycle pathways. This hypothesis is further corroborated both by the significantly higher ABA concentrations that we measured in *VvGST40*-primed plants under NS conditions and by the fact that, in comparison with

untreated plants, ABA accumulation in *VvGST40* samples followed a much stronger increase during the drought spell.

Drought stress is strictly connected with *de novo* ABA synthesis (in both leaves and roots) leading to a complex network of ABA-mediated responses and signaling cascades largely studied so far (*e.g.* Xiong & Zhu, 2003; Nambara & Marion-Poll, 2005; McAdam *et al.*, 2016; Sah *et al.*, 2016; McAdam & Brodribb, 2018). Under drought, ABA levels are regulated by two main mechanisms: i) the *de novo* biosynthesis, mainly dependent on the 9-cis-epoxy carotenoid dioxygenase (NCED) activity, and ii) the de-glycosylation of the ABA inactive form (ABA-GE). At transcriptional level, *NCED* is one of the main genes responsible for the *de novo* ABA biosynthesis and is commonly used as a marker of stress in many crops. The fact that *VvNCED3* expression was already upregulated at T2 in *VvGST40* WS samples supports the SIGS-mediated priming effect emerging from the measurement of physiological parameters. Moreover, as well as ABA accumulation trends, *VvNCED3* expression profiles showed a negative correlation with g_s rates in WS samples (at T2 and T4), as previously reported for *Vitis vinifera* cv. Shiraz by Soar *et al.* (2004).

As cited before, ABA quantity and activity not only depend on the *de novo* biosynthesis of the hormone, but they also rely on the mobilization of the inactive ABA form (ABA-glucosyl ester, ABA-GE) *via* hydrolyzation, which represents an alternative reservoir of the hormone. ABA-GE is mainly hydrolyzed by the activity of beta-glucosidases (BG), which are located at the endoplasmic reticulum level. Here we showed that at the transcriptional level both the *de novo* ABA biosynthesis promoted by *VvNCED3* (already at T2) and the de-glycosylation of ABA-GE promoted by the activity of *VvBG1* were strongly active at T4 in *VvGST40* WS plants. Accordingly, Lee et al. (2006) demonstrated the *AtBG1*-mediated increase of the active ABA form from ABA-GE in Arabidopsis plants subjected to water stress. This represents a time and energy-saving way for the plant to mobilize active ABA, a strategy that is particularly useful during abiotic stress exposure (Long *et al.*, 2019). Collectively, these findings suggested that *VvGST40*-primed plants were able to better adapt to drought stress effects as they were prompter than the others to produce the active ABA form by finely tuning both pathways regulating ABA biosynthesis. However, stomata closure is actively regulated by hydraulic and chemical signals, and ABA signaling could have more than one role in the

control of abiotic stress response. To deepen this subject, the key ABA catabolism-related genes were also evaluated in response to the diverse treatments applied. The expression of the ABA-Glucosyltransferase (*VvGT*), responsible for ABA degradation through conjugation with a glycosyl group (Xu *et al.*, 2013), did not change during the experimental time course regardless of SIGS application, suggesting that this catabolic pathway was not relevant for the plant, at least in our experimental conditions. Conversely, *VvHYD1* was up-regulated already under irrigation and particularly in *VvGST40* plants, further supporting the observation that under WS the primed plants react earlier and faster than the others in terms of ABA concentration and biosynthesis, triggering responses that are commonly activated during the late stages of prolonged drought (Perrone *et al.*, 2012; Belfiore *et al.*, 2021). Additionally, in *VvGST40* plants subjected to WS, the β-glucosidase-encoding gene *VvBG1* was expressed more than two orders of magnitude than *VvHYD1*, revealing a likely relevant contribution of the de-conjugation reaction to free ABA levels.

The different timing in the reprogramming of ABA metabolic and signaling related genes observed in *VvGST40* plants was further evidenced by the analysis of transcripts involved in ABA sensing (i.e. *VvabaR* and *VvPP2C4*) and signaling (i.e. *VvABF1*). All those transcripts, and particularly *PP2C4*, were activated in *VvGST40* vines before the occurrence of severe water stress. Accordingly, in Boneh *et al.* (2012), *VvPP2C4* was defined as one of the major interacting partners for grape ABA receptors and its increased expression in *VvGST40* WS samples at T2 and T4 was consistent with the observed ABA concentration trend. The same authors also analyzed the expression profiles of *VvABF1* and *VvPP2C4* in plants subjected to different abiotic stresses, including drought, and reported a marked up-regulation of *VvPP2C4* in contrast to *VvABF1* (Boneh *et al.* 2012a,b).

Additionally, the RT-qPCR data indicated that, although at lesser extent, ABA was also perceived in CTRL and *GFP* plants upon severe water stress (T2), thus suggesting that the quick failure in g_s and Pn rates observed in these plants was mainly hydraulic-mediated, as previously reported (Belfiore *et al.*, 2021).

These results, together with the *de novo* ABA synthesis mediated by *VvNCED3*, could explain the increased stress resistance and the longer recovery phase of *VvGST40* WS plants with respect to the CTRL WS and *GFP* WS ones.

4.3 Cross-talk between ABA and strigolactone pathways reinforces drought tolerance mechanisms in *VvGST40*-primed plants

Among carotenoid-derived compounds, strigolactones (SLs) were recently designated as a new class of phytohormones exuded from the roots and involved in the early dialogue between roots and arbuscular mycorrhizal fungi (AMF) inducing the so-called pre-symbiotic stage (Fernández *et al.*, 2019). Furthermore, SLs were found to play pivotal roles in several plant developmental processes (e.g. shoot branching and root architecture) and positively regulate plant responses to drought stress in several crops, including grapevine (Mishra *et al.*, 2017; Cochetel *et al.*, 2018; Min *et al.*, 2019). The SL biosynthesis derives from carotenoids through sequential cleavage steps mediated by CCD7 and CCD8 dioxygenases, whose encoding genes have also been functionally characterized in grapevine (*VvCCD7* and *VvCCD8*, respectively) both *in vitro* and *in vivo* (Cochetel *et al.*, 2018). In Arabidopsis, the CCD family includes several members annotated as NCEDs involved in the ABA biosynthesis (Auldridge *et al.*, 2006) and leading to a strict correlations between SLs and ABA, especially in response to biotic and abiotic stressful conditions (Mishra *et al.*, 2017).

To provide further insights into the molecular signals putatively associated with the delayed stomatal closure and photosynthetic inhibition at the basis of *VvGST40* plants drought tolerance, we analyzed expression changes of the SL biosynthetic genes *VvCCD7* and *VvCCD8*. Although both genes were up-regulated following drought imposition independently of SIGS application, the highest transcriptional levels were observed in *VvGST40* WS plants. Consistently, rooted cuttings of Cabernet Sauvignon subjected to water deficit displayed higher concentration of foliar ABA and SLs accompanied by the up-regulation of their biosynthetic genes (*VvNCED*, *VvCCD7* and *VvCCD8* respectively) (Min *et al.*, 2019). The authors also observed an improved drought tolerance of the cuttings pre-treated with GR24, a synthesized strigolactone that primes the antioxidant system and ABA metabolism alleviating the drought adverse effects.

These findings suggest that the improved physiological performances of *VvGST40*-primed plants could rely on the ability of these plants to activate ABA metabolism and transcription of the SL biosynthetic genes involved in the ABA crosstalk before the occurrence of a severe drought condition. Notably, the potential increase in SL

accumulation can positively influence AMF recruiting in these plants, thereby promoting functional symbioses that are helpful to withstand stressful conditions (Chitarra *et al.*, 2016; Ruiz-Lozano *et al.*, 2016; Irankhah *et al.*, 2020b).

4.4 The SIGS treatment affects the modulation of Ascorbate-Glutathione cycle (Asc-GSH)-related genes and patterns of resveratrol accumulation

Ascorbate peroxidase (APX) is a thylakoid-bound and stromal soluble enzyme with a known role in H_2O_2 metabolism (Foyer & Noctor, 2011). In both herbaceous and woody species, *APX* is commonly up regulated in response to drought, both by transcriptional and post-transcriptional mechanisms (Laxa *et al.*, 2019). Our data indicated that Nevertheless, Wang *et al*. (2019) did not report significant changes in *VvAPX* expression in water stressed Cabernet Sauvignon plants, likely due to different genotype-dependent responses and experimental conditions. Besides APX, also the transcriptional rates of the glutathione reductase encoding gene (*GR*) increased in *VvGST40* plants along with the progression of drought stress. Accordingly, Laxa *et al*. (2019) investigated the modulation of several genes encoding enzymes involved in the Asc-GSH cycle and reported a strong activation of *GR* in both herbaceous and woody species upon prolonged drought stress conditions. It must be noticed, however, that the induction of *GR* transcription occurred earlier in *GFP* WS than *GST40* plants showing a similar profile to that of *VvDHAR* and *VvMDHAR*, thereby leading to the hypothesis of a ROS scavenging cycle activation mainly in response to the application of dsRNAs targeting an exogenous gene (GFP). Accordingly, Niehl *et al*. (2016) demonstrated that treatment with exogenous dsRNA molecules (e.g. *GFP*) induced pattern-triggered immunity (PTI) responses in Arabidopsis, in turn triggering a burst of reactive oxygen species (ROS) that potentially requires the activation of the Asc-GSH cycle for ROS detoxification.

Besides Asc-GSH cycle, the protection against oxidative stress and ROS generation is also achieved in plants through the synthesis and accumulation of antioxidant secondary metabolites. Among these, resveratrol, a monomeric stilbene, is one of the major antioxidant compounds in grapevine, whose biosynthesis can be induced by many biotic and abiotic stresses, including drought (Chitarra *et al*., 2017; Dubrovina & Kiselev, 2017). For instance, the induction of osmotic stress in polyethylene glycol- and sucrose-treated Chardonnay leaves led to the accumulation of *t*-resveratrol up to 3 µg g^{-1} DM and to the up-regulation of both ABA and stilbene

biosynthetic genes (Hatmi *et al.*, 2014). In addition, Nicolas *et al.* (2014) suggested an active role of ABA in the regulation of resveratrol biosynthesis by reporting an increase of *VvABF2* transcripts in grapevine cells coupled with strong stilbene concentrations. The same authors also demonstrated that the application of exogenous ABA is sufficient to increase *t*-resveratrol levels in non-transgenic grapevine cells (Nicolas *et al.*, 2014). In this line, the high quantity of both ABA and *t*-resveratrol measured at T4 in *VvGST40* WS plants, consistently with the higher transcriptional rates of *VvSTS1* gene, confirmed the strict correlation between ABA and stilbenoid accumulation pathways in grapevine.

Collectively, in severely droughted *VvGST40*-primed plants the accumulation of the antioxidant compound resveratrol coupled with the activation of ABA, SL and ROS scavenging pathways provides further support for the observed delay in photosynthesis failure and stomata closure. Such a response could most likely underpin the increased stress tolerance of *VvGST40*-primed plants. More in detail, the downregulation of the specific *VvGST40* isoform, homologue of *AtGSTU17*, provides new information on the biological function of GST in grapevine, highlighting molecular, biochemical and physiological responses that confirm what previously observed in Arabidopsis (Chen *et al.*, 2012).

5. Conclusion

Here, we used the innovative SIGS technique to functionally characterize a grapevine putative glutathione-S-transferase (*VvGST40*) gene, homologue to the Arabidopsis *AtGSTU17* whose mutant lines showed improved drought and salt stress resistance. To the best of our knowledge, this is the first study in which the SIGS approach has successfully been applied to target an endogenous gene conferring abiotic stress resistance in a woody crop (*i.e.* grapevine) recalcitrant to traditional functional genetics protocols.

Silencing of the target endogenous gene was successfully achieved triggering priming effects in *VvGST40*-treated plants, which indeed showed an improved resilience when submitted to severe water stress treatment. Notably, once re-watered, the *VvGST40*-treated plants recovered very slowly with respect to the CTRL and *GFP* ones. Moreover, the *VvGST40* WS plants did fully recover, showing a phenotype similar to non-stressed plants, without any evident damage due to the experienced drought conditions (Fig.

6c,d). To deepen the molecular responses mediated by the downregulation of *VvGST40* we analyzed the expression pattern of target genes involved in the ABA biosynthesis, catabolism and signaling. Indeed, *VvGST40*-treated plants slowed the kinetics of the metabolic, ABA-related control of stomatal closure and re-opening. This outcome, coupled with the analysis of target metabolites and antioxidant- and ABA-related transcripts, confirmed that *VvGST40*-treated plants were in a priming status compared with controls, indicating that glutathione S-transferase plays a pivotal role in controlling drought resilience in grapevines. These results offer new insights into the biological functions of GST in grapevine, adding information on the negative role that *VvGST40* plays during the drought stress response.

Collectively, these findings further confirmed the potentiality of SIGS, evidencing the reliability of this technique not only for plant protection purposes but also for functional genomics approaches, such as the study of resilience mechanisms to drought here reported.

Acknowledgements

This work was founded by the Italian Ministry of Agriculture Food and Forestry (MIPAAF) in the framework of the BIOTECH-VITECH project.

Author contributions

LN and WC designed research. LN, WC, MG and MDR performed research. WC, LN and CP analyzed the data. WC, MG and LN wrote the manuscript. CL and CP provided critical feedback and helped interpreting the results. All authors contributed to revisions and gave final approval for publication.

ORCID

Luca Nerva: https://orcid.org/0000-0001-5009-5798

Chiara Pagliarani: https://orcid.org/0000-0003-4656-6192

Mirko De Rosso: https://orcid.org/0000-0003-4005-7012

Claudio Lovisolo: https://orcid.org/0000-0001-8825-2904

Walter Chitarra: https://orcid.org/0000-0002-5382-3794

Conflict of Interest

The authors have no conflict of interest.

Data availability statement

The data that supports the findings of this study are available in the supplementary material of this article.

Figures

Fig. 1 *VvGST40* expression changes, and relative *GFP* dsRNA quantity and persistence during the experimental time course. (a) Schematic representation of the dsRNAs position used in the present study. On the left side, dsRNAs design on the *VvGST40* gene covering 688 bp at 5'-end of the open reading frame. On the right side, dsRNAs design (376 bp) on the *eGFP* sequence amplified from the pCBCT plasmid as previously reported (Nerva et al., 2020); **(b)** *VvGST40* expression level and **(c)** *GFP* dsRNA relative quantity. Relative *VvGST40* transcript abundance in leaves of *VvGST40* dsRNA-treated plants (diamonds, red dotted lines), *GFP* dsRNA-treated plants (triangles, green dashed lines) and controls (CTRL, circles, black line) either submitted (WS, empty symbols) or not (NS, filled symbols) to water stress. All data are expressed as means ± SD (n = 3). For each experimental day, different letters denote significant differences according to the Tukey's HSD test ($P \leq 0.05$), while asterisks above bars mark significant differences according to the Student's *t*-test ($P \leq 0.05$).

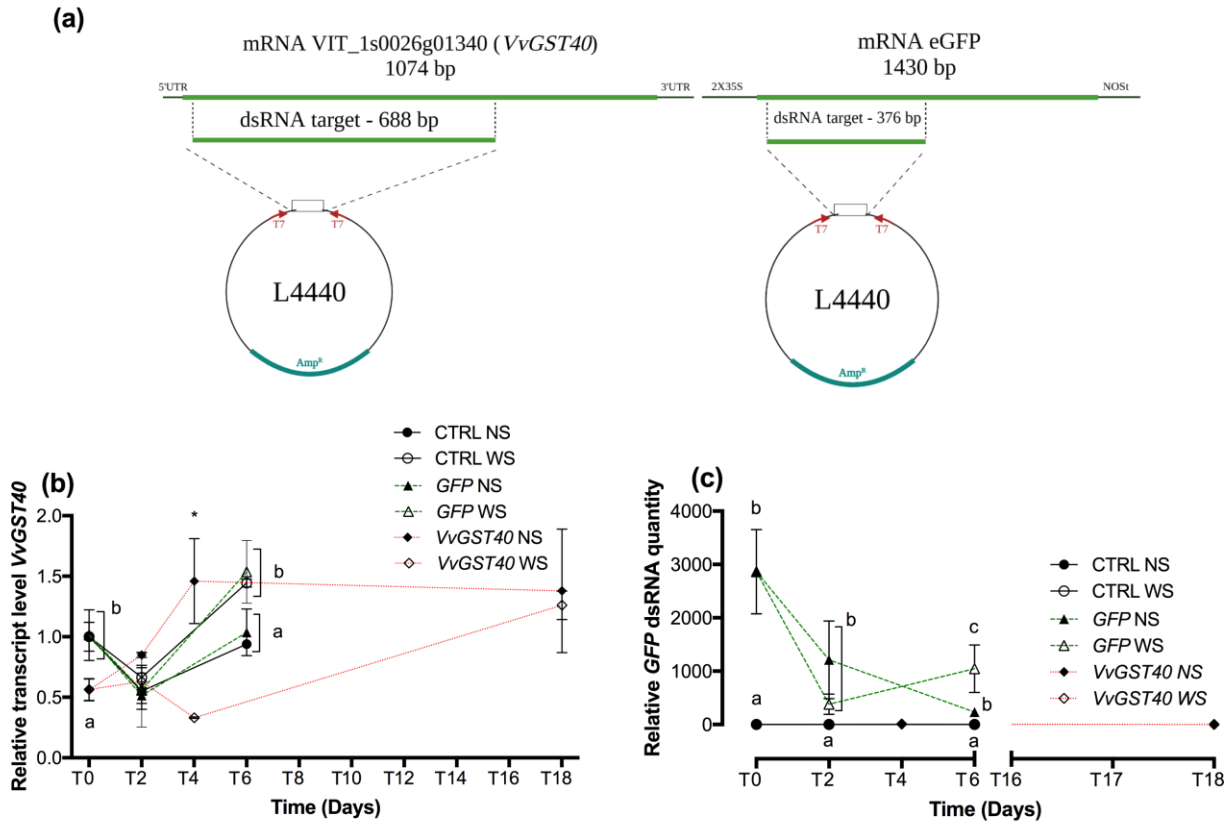

Fig. 2 Leaf gas exchange over time. Measurements of **(a)** Stomatal conductance (g_s); **(b)** net photosynthesis (Pn) and **(c)** intercellular CO_2 (Ci) were performed on leaves of *VvGST40* dsRNA-treated plants (diamonds, red dotted lines), *GFP* dsRNA-treated plants (triangles, green dashed lines) and controls (CTRL, circles, black line) either submitted (WS, empty symbols) or not (NS, filled symbols) to water stress. All data are expressed as means ± SD (n = 4). For each experimental day, different letters denote significant differences according to the Tukey's HSD test ($P \leq 0.05$), while asterisks above bars mark significant differences according to the Student's *t*-test ($P \leq 0.05$).

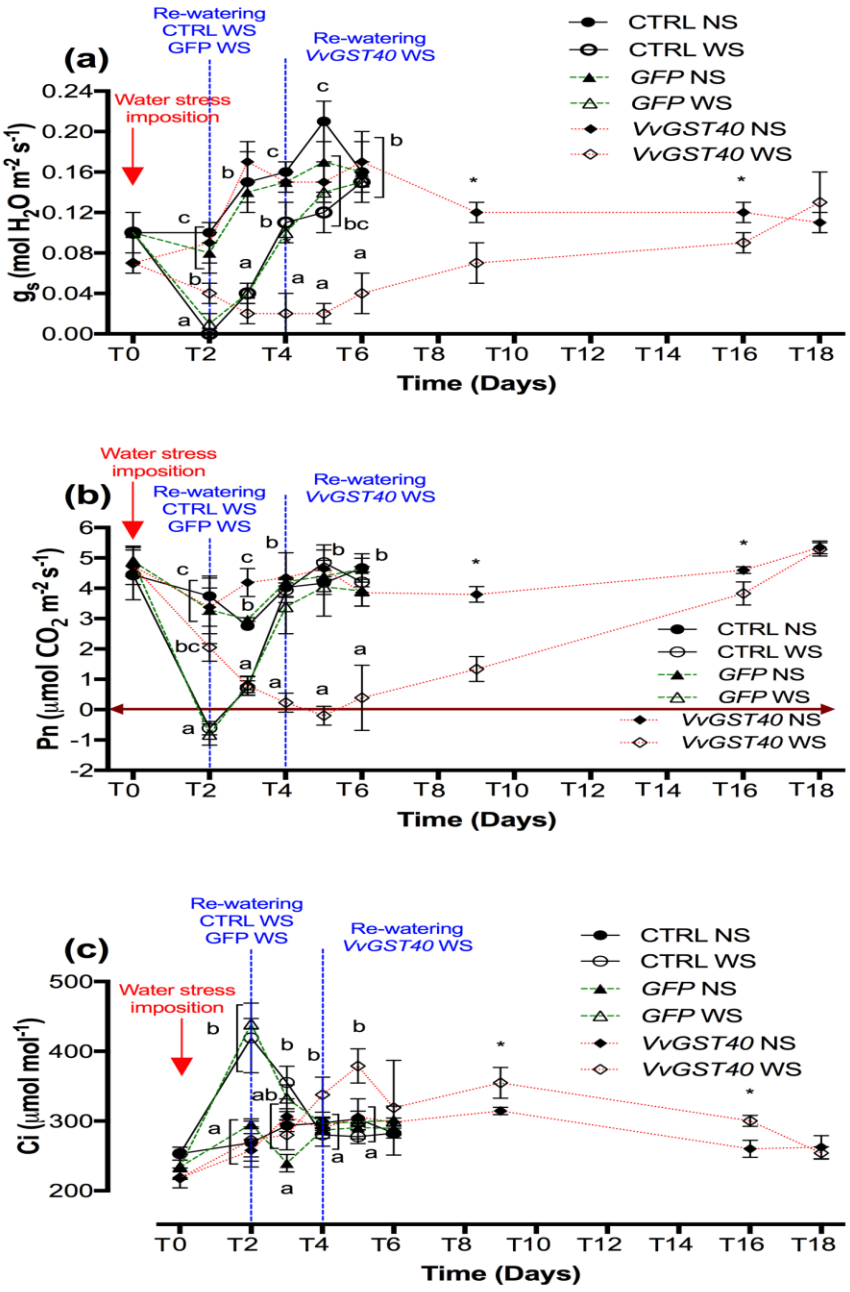

Fig. 3 Leaf ABA concentration and expression changes of ABA-related genes over time. Endogenous leaf ABA concentration (**a**) and relative transcript abundance of **(b)** *VvNCED3*; **(c)** *VvBG1*; **(d)** *VvGT*; **(e)** *VvHYD1*; **(f)** *VvabaR* (PYR-8 like); **(g)** *VvPP2C4* and **(h)** *VvABF1* in leaves of *VvGST40* dsRNA-treated plants, *GFP* dsRNA-treated plants and controls (CTRL) either submitted (WS) or not (NS) to water stress. All data are expressed as means ± SD (n = 3). For each experimental day, different letters denote significant differences according to the Tukey's HSD test ($P \leq 0.05$), while asterisks above bars mark significant differences according to the Student's *t*-test ($P \leq 0.05$).

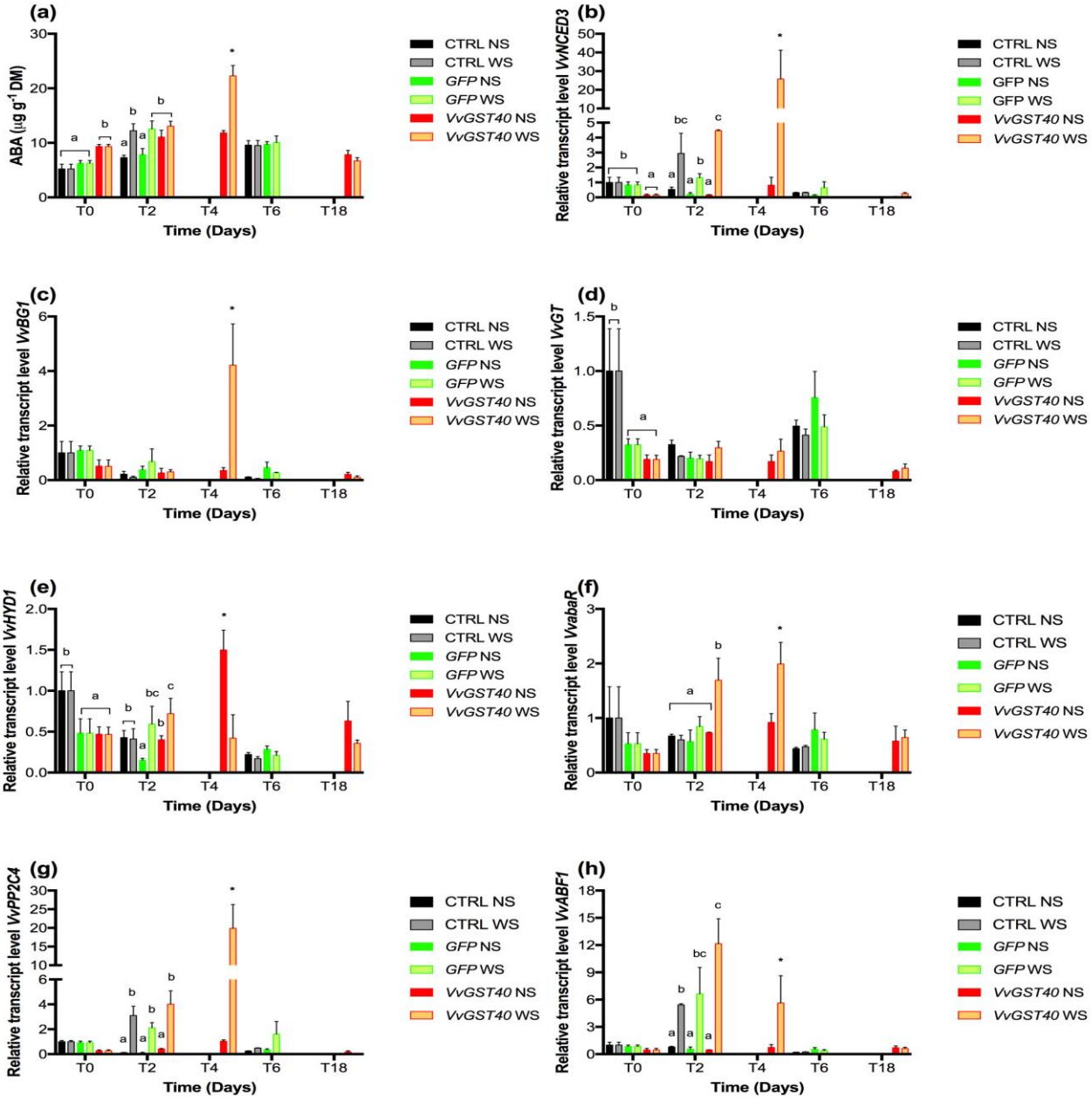

Fig. 4 Expression changes of strigolactone biosynthetic-related genes over time. Relative transcript abundance of **(a)** *VvCCD7* and **(b)** *VvCCD8* in leaves of *VvGST40* dsRNA-treated plants, *GFP* dsRNA-treated plants and controls (CTRL) either submitted (WS) or not (NS) to water stress. For each experimental day, different letters denote significant differences according to the Tukey's HSD test ($P \leq 0.05$), while asterisks above bars mark significant differences according to the Student's *t*-test ($P \leq 0.05$).

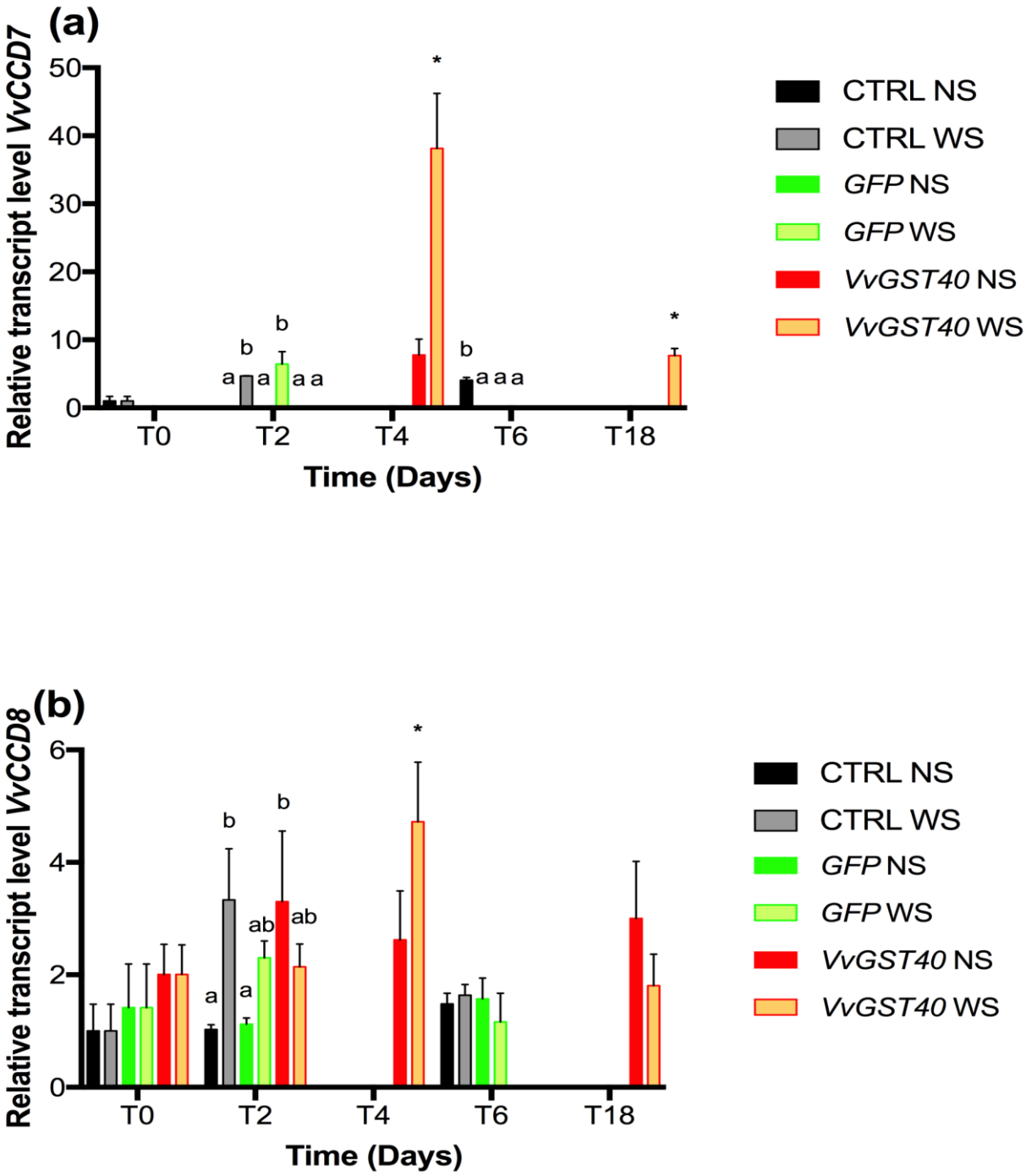

Fig. 5 Expression changes of antioxidant-related genes over time. Relative transcript abundance of **(a)** *VvAPX*; **(b)** *VvGR*; **(c)** *VvDHAR* and **(d)** *VvMDHAR* in leaves of *VvGST40* dsRNA-treated plants, *GFP* dsRNA-treated plants and controls (CTRL) either submitted (WS) or not (NS) to water stress. For each experimental day, different letters denote significant differences according to the Tukey's HSD test ($P \leq 0.05$), while asterisks above bars mark significant differences according to the Student's *t*-test ($P \leq 0.05$).

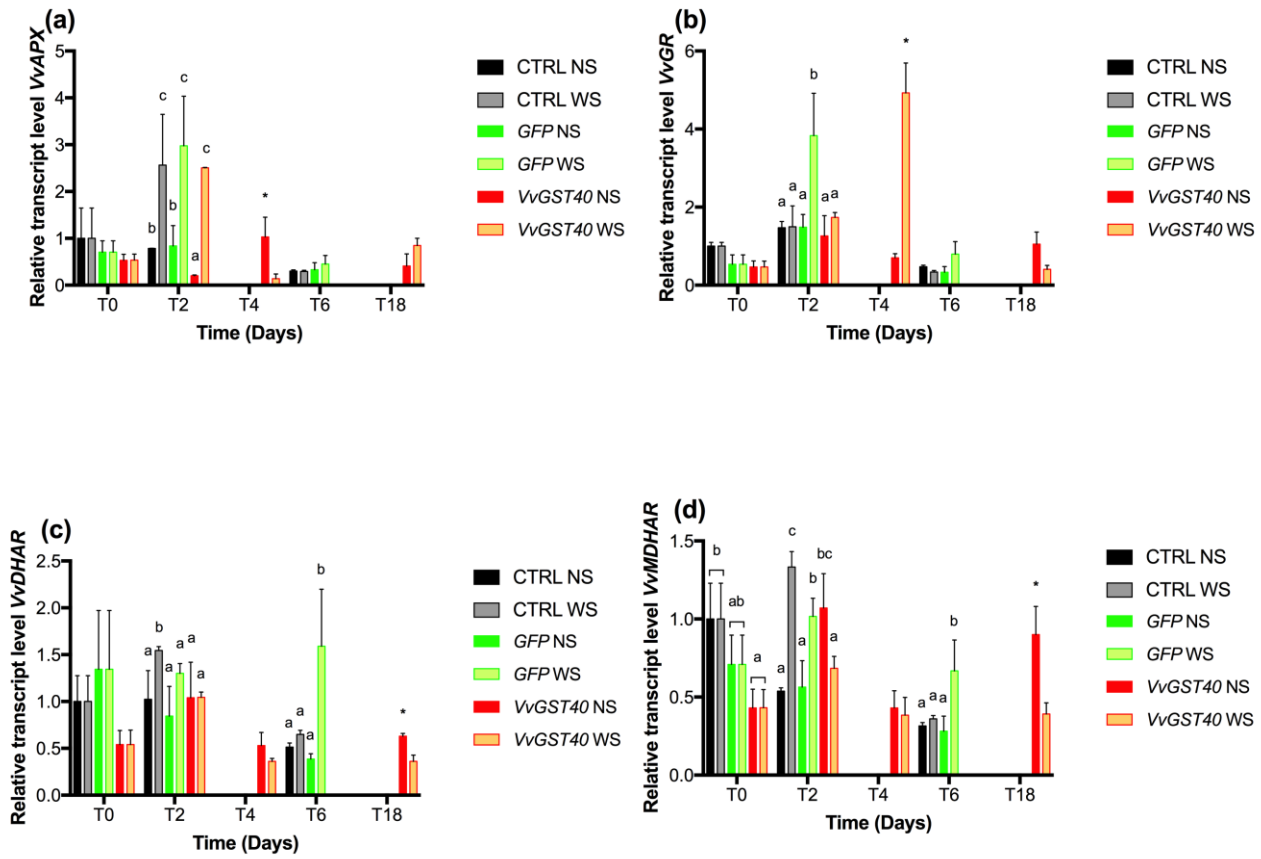

Fig. 6 Resveratrol concentration in leaf and expression changes of a stilbene biosynthetic gene over time. Examples of phenotypic status in recovered plants. Relative transcript abundance of *VvSTS1* in leaves of *VvGST40* dsRNA-treated plants, *GFP* dsRNA-treated plants and controls (CTRL) either submitted (WS) or not (NS) to water stress. **(a)** *trans*-resveratrol concentration in leaves and **(b)** *VvSTS1*. For each experimental day, different letters denote significant differences according to the Tukey's HSD test ($P \leq 0.05$) while asterisks above bars mark significant differences according to the Student's *t*-test ($P \leq 0.05$). **(c)** and **(d)** examples of recovered CTRL WS and *GFP* WS plants phenotypes in comparison with *VvGST40* WS recovered ones.

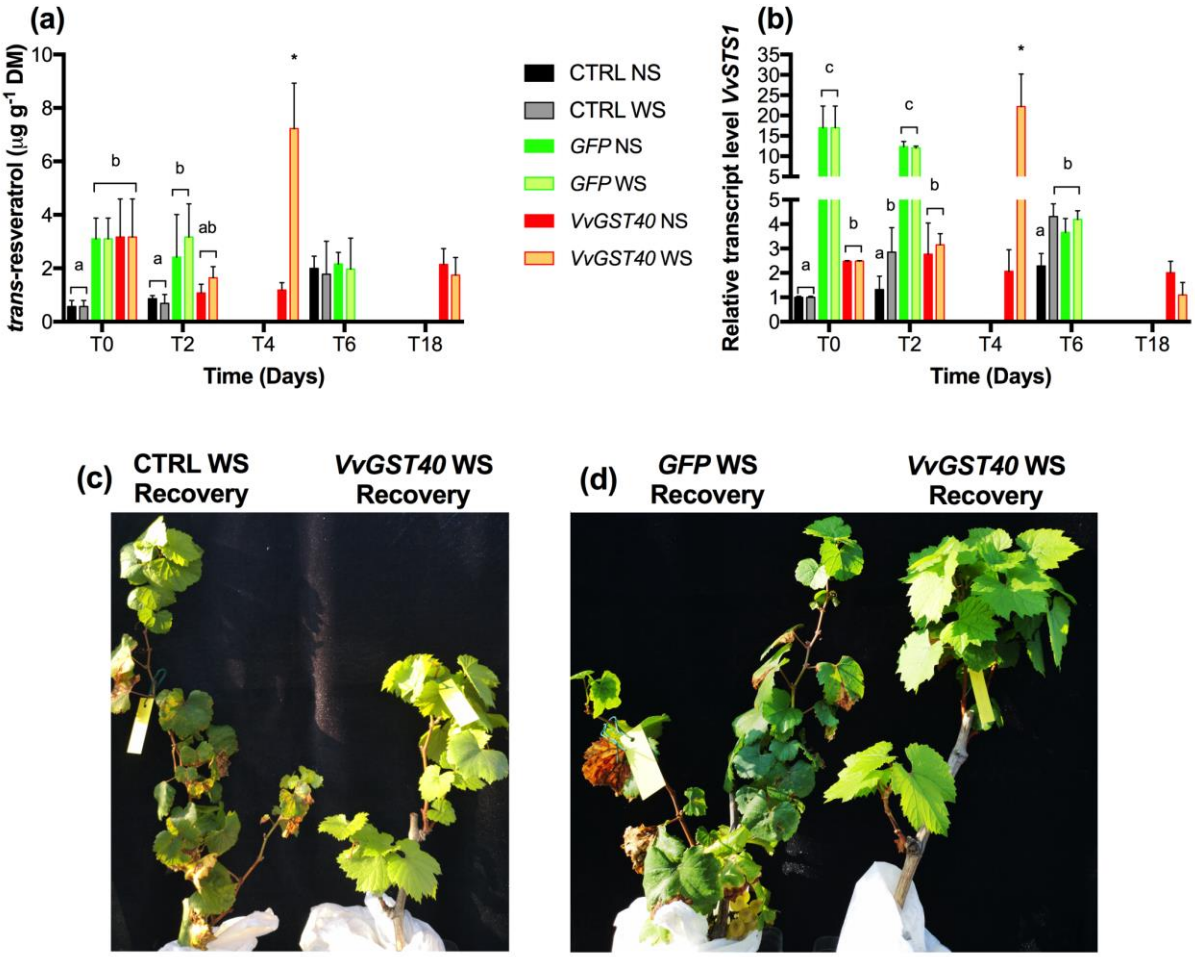

References

Ahn S-J, Donahue K, Koh Y, Martin RR, Choi M-Y. **2019**. Microbial-Based Double-Stranded RNA Production to Develop Cost-Effective RNA Interference Application for Insect Pest Management. *International Journal of Insect Science* **11**: 117954331984032.

Auldridge ME, McCarty DR, Klee HJ. **2006**. Plant carotenoid cleavage oxygenases and their apocarotenoid products. *Current opinion in plant biology* **9**: 315–321.

Belfiore N, Nerva L, Fasolini R, Gaiotti F, Lovat L, Chitarra W. **2021**. Leaf gas exchange and abscisic acid in leaves of Glera grape variety during drought and recovery. *Theoretical and Experimental Plant Physiology*: 1–10.

Boneh U, Biton I, Schwartz A, Ben-Ari G. **2012a**. Characterization of the ABA signal transduction pathway in *Vitis vinifera*. *Plant Science* **187**: 89–96.

Boneh U, Biton I, Zheng C, Schwartz A, Ben-Ari G. **2012b**. Characterization of potential ABA receptors in *Vitis vinifera*. *Plant cell reports* **31**: 311–321.

Chen J-H, Jiang H-W, Hsieh E-J, Chen H-Y, Chien C-T, Hsieh H-L, Lin T-P. **2012**. Drought and salt stress tolerance of an Arabidopsis glutathione S-transferase U17 knockout mutant are attributed to the combined effect of glutathione and abscisic acid. *Plant Physiology* **158**: 340–351.

Chitarra W, Cuozzo D, Ferrandino A, Secchi F, Palmano S, Perrone I, Boccacci P, Pagliarani C, Gribaudo I, Mannini F. **2018**. Dissecting interplays between Vitis vinifera L. and grapevine virus B (GVB) under field conditions. *Molecular plant pathology* **19**: 2651–2666.

Chitarra W, Pagliarani C, Maserti B, Lumini E, Siciliano I, Cascone P, Schubert A, Gambino G, Balestrini R, Guerrieri E. **2016**. Insights on the impact of arbuscular mycorrhizal symbiosis on tomato tolerance to water stress. *Plant Physiology* **171**: 1009–1023.

Cochetel N, Météier E, Merlin I, Hévin C, Pouvreau J-B, Coutos-Thévenot P, Hernould M, Vivin P, Cookson SJ, Ollat N. **2018**. Potential contribution of strigolactones in regulating scion growth and branching in grafted grapevine in response to nitrogen availability. *Journal of experimental botany* **69**: 4099–4112.

Dalakouras A, Wassenegger M, Dadami E, Ganopoulos I, Pappas ML, Papadopoulou K. **2020**. Genetically modified organism-free RNA interference: exogenous application of RNA molecules in plants. *Plant physiology* **182**: 38–50.

Dubrovina AS, Aleynova OA, Kalachev AV, Suprun AR, Ogneva ZV, Kiselev KV. **2019**. Induction of Transgene Suppression in Plants via External Application of Synthetic dsRNA. *International Journal of Molecular Sciences* **20**: 1585.

Fernández I, Cosme M, Stringlis IA, Yu K, de Jonge R, van Wees SM, Pozo MJ, Pieterse CM, van der Heijden MG. **2019**. Molecular dialogue between arbuscular mycorrhizal fungi and the nonhost plant Arabidopsis thaliana switches from initial detection to antagonism. *New Phytologist* **223**: 867–881.

Ferrandino A, Lovisolo C. **2014**. Abiotic stress effects on grapevine (*Vitis vinifera* L.): Focus on abscisic acid-mediated consequences on secondary metabolism and berry quality. *Environmental and Experimental Botany* **103**: 138–147.

Fischer BB, Hideg E, Krieger-Liszkay A. **2013**. Production, detection, and signaling of singlet oxygen in photosynthetic organisms. *Antioxidants & redox signaling* **18**: 2145–2162.

Flexas J, Escalona JM, Evain S, Gulías J, Moya I, Osmond CB, Medrano H. **2002**. Steady-state chlorophyll fluorescence (Fs) measurements as a tool to follow variations of net CO2 assimilation and stomatal conductance during water-stress in C3 plants. *Physiologia plantarum* **114**: 231–240.

Foyer CH, Noctor G. **2005**. Redox homeostasis and antioxidant signaling: a metabolic interface between stress perception and physiological responses. *The Plant Cell* **17**: 1866–1875.

Foyer CH, Noctor G. **2009**. Redox regulation in photosynthetic organisms: signaling, acclimation, and practical implications. *Antioxidants & redox signaling* **11**: 861–905.

Foyer CH, Noctor G. **2011**. Ascorbate and glutathione: the heart of the redox hub. *Plant physiology* **155**: 2–18.

Gambino G, Gribaudo I. **2012**. Genetic transformation of fruit trees: current status and remaining challenges. *Transgenic research* **21**: 1163–1181.

Giudice G, Moffa L, Varotto S, Cardone M, Bergamini C, De Lorenzis G, Velasco R, Nerva L, Chitarra W. **2021**. Novel and emerging biotechnological crop protection approaches. *Plant Biotechnology Journal*.

Hannon GJ. **2002**. RNA interference. *nature* **418**: 244–251.

Hatmi S, Trotel-Aziz P, Villaume S, Couderchet M, Clément C, Aziz A. **2014**. Osmotic stress-induced polyamine oxidation mediates defence responses and reduces stress-enhanced grapevine susceptibility to *Botrytis cinerea*. *Journal of experimental botany* **65**: 75–88.

Irankhah S, Chitarra W, Nerva L, Antoniou C, Lumini E, Volpe V, Ganjeali A, Cheniany M, Mashreghi M, Fotopoulos V. **2020a**. Impact of an arbuscular mycorrhizal fungal inoculum and exogenous MeJA on fenugreek secondary metabolite production under water deficit. *Environmental and Experimental Botany*: 104096.

Irankhah S, Sillo F, Nerva L, Ganjeali A, Balestrini R, Chitarra W. **2020b**. Combined effects of water deficit, exogenous ethylene application and root symbioses on Trigonelline and ABA accumulation in fenugreek. *Applied Sciences* **10**: 2338.

Kalantidis K, Schumacher HT, Alexiadis T, Helm JM. **2008**. RNA silencing movement in plants. *Biology of the Cell* **100**: 13–26.

Kim VN. **2008**. Sorting out small RNAs. *Cell* **133**: 25–26.

Kiselev KV, Suprun AR, Aleynova OA, Ogneva ZV, Dubrovina AS. **2021a**. Physiological Conditions and dsRNA Application Approaches for Exogenously induced RNA Interference in *Arabidopsis thaliana*. *Plants* **10**: 264.

Kiselev KV, Suprun AR, Aleynova OA, Ogneva ZV, Kalachev AV, Dubrovina AS. **2021b**. External dsRNA Downregulates Anthocyanin Biosynthesis-Related Genes and Affects Anthocyanin Accumulation in *Arabidopsis thaliana*. *International Journal of Molecular Sciences* **22**: 6749.

Kusaba M. **2004**. RNA interference in crop plants. *Current opinion in Biotechnology* **15**: 139–143.

Kushiro T, Okamoto M, Nakabayashi K, Yamagishi K, Kitamura S, Asami T, Hirai N, Koshiba T, Kamiya Y, Nambara E. **2004**. The Arabidopsis cytochrome P450 CYP707A encodes ABA 8′-hydroxylases: key enzymes in ABA catabolism. *The EMBO journal* **23**: 1647–1656.

Labudda M, Safiul Azam FM. **2014**. Glutathione-dependent responses of plants to drought: a review.

Lau S-E, Schwarzacher T, Othman RY, Harikrishna JA. **2015**. dsRNA silencing of an R2R3-MYB transcription factor affects flower cell shape in a Dendrobium hybrid. *BMC plant biology* **15**: 1–14.

Li H, Guan R, Guo H, Miao X. **2015**. New insights into an RNAi approach for plant defence against piercing-sucking and stem-borer insect pests. *Plant, cell & environment* **38**: 2277–2285.

Lionello P, Malanotte-Rizzoli P, Boscolo R, Alpert P, Artale V, Li L, Luterbacher J, May W, Trigo R, Tsimplis M. **2006**. The Mediterranean climate: an overview of the main characteristics and issues.

Long H, Zheng Z, Zhang Y, Xing P, Wan X, Zheng Y, Li L. **2019**. An abscisic acid (ABA) homeostasis regulated by its production, catabolism and transport in peanut leaves in response to drought stress. *Plos one* **14**: e0213963.

Lovisolo C, Lavoie-Lamoureux A, Tramontini S, Ferrandino A. **2016**. Grapevine adaptations to water stress: new perspectives about soil/plant interactions. *Theoretical and Experimental Plant Physiology* **28**: 53–66.

Lovisolo C, Perrone I, Carra A, Ferrandino A, Flexas J, Medrano H, Schubert A. **2010**. Drought-induced changes in development and function of grapevine (*Vitis* spp.) organs and in their hydraulic and non-hydraulic interactions at the whole-plant level: a physiological and molecular update. *Functional plant biology* **37**: 98–116.

Lück S, Kreszies T, Strickert M, Schweizer P, Kuhlmann M, Douchkov D. **2019**. siRNA-Finder (si-Fi) software for RNAi-target design and off-target prediction. *Frontiers in Plant Science* **10**: 1023.

Marcianò D, Ricciardi V, Fassolo EM, Passera A, Bianco PA, Failla O, Casati P, Maddalena G, De Lorenzis G, Toffolatti SL. **2021**. RNAi of a putative grapevine

susceptibility gene as a possible downy mildew control strategy. *Frontiers in plant science* **12**.

McAdam SA, Brodribb TJ. **2018**. Mesophyll cells are the main site of abscisic acid biosynthesis in water-stressed leaves. *Plant Physiology* **177**: 911–917.

McAdam SA, Brodribb TJ, Ross JJ. **2016**. Shoot-derived abscisic acid promotes root growth. *Plant, cell & environment* **39**: 652–659.

Medrano H, Escalona JM, Bota J, Gulías J, Flexas J. **2002**. Regulation of photosynthesis of C3 plants in response to progressive drought: stomatal conductance as a reference parameter. *Annals of botany* **89**: 895–905.

Min Z, Li R, Chen L, Zhang Y, Li Z, Liu M, Ju Y, Fang Y. **2019**. Alleviation of drought stress in grapevine by foliar-applied strigolactones. *Plant Physiology and Biochemistry* **135**: 99–110.

Mishra S, Upadhyay S, Shukla RK. **2017**. The role of strigolactones and their potential cross-talk under hostile ecological conditions in plants. *Frontiers in physiology* **7**: 691.

Mitter N, Worrall EA, Robinson KE, Li P, Jain RG, Taochy C, Fletcher SJ, Carroll BJ, Lu GM, Xu ZP. **2017**. Clay nanosheets for topical delivery of RNAi for sustained protection against plant viruses. *Nature plants* **3**: 16207.

Nambara E, Marion-Poll A. **2005**. Abscisic acid biosynthesis and catabolism. *Annu. Rev. Plant Biol.* **56**: 165–185.

Nerva L, Sandrini M, Gambino G, Chitarra W. **2020**. Double-Stranded RNAs (dsRNAs) as a Sustainable Tool against Gray Mold (*Botrytis cinerea*) in Grapevine: Effectiveness of Different Application Methods in an Open-Air Environment. *Biomolecules* **10**: 200.

Nicolas P, Lecourieux D, Kappel C, Cluzet S, Cramer G, Delrot S, Lecourieux F. **2014**. The basic leucine zipper transcription factor ABSCISIC ACID RESPONSE ELEMENT-BINDING FACTOR2 is an important transcriptional regulator of abscisic acid-dependent grape berry ripening processes. *Plant Physiology* **164**: 365–383.

Numata K, Ohtani M, Yoshizumi T, Demura T, Kodama Y. **2014**. Local gene silencing in plants via synthetic ds RNA and carrier peptide. *Plant biotechnology journal* **12**: 1027–1034.

Pagliarani C, Moine A, Chitarra W, Meloni GR, Abbà S, Nerva L, Pugliese M, Gullino ML, Gambino G. **2020**. The Molecular Priming of Defense Responses is Differently Regulated in Grapevine Genotypes Following Elicitor Application against Powdery Mildew. *International journal of molecular sciences* **21**: 6776.

Perrone I, Pagliarani C, Lovisolo C, Chitarra W, Roman F, Schubert A. **2012**. Recovery from water stress affects grape leaf petiole transcriptome. *Planta* **235**: 1383–1396.

Reinhart BJ, Weinstein EG, Rhoades MW, Bartel B, Bartel DP. **2002**. MicroRNAs in plants. *Genes & development* **16**: 1616–1626.

Ruiz-Lozano JM, Aroca R, Zamarreño ÁM, Molina S, Andreo-Jiménez B, Porcel R, García-Mina JM, Ruyter-Spira C, López-Ráez JA. **2016**. Arbuscular mycorrhizal symbiosis induces strigolactone biosynthesis under drought and improves drought tolerance in lettuce and tomato. *Plant, cell & environment* **39**: 441–452.

Sah SK, Reddy KR, Li J. **2016**. Abscisic acid and abiotic stress tolerance in crop plants. *Frontiers in plant science* **7**: 571.

Seleiman MF, Al-Suhaibani N, Ali N, Akmal M, Alotaibi M, Refay Y, Dindaroglu T, Abdul-Wajid HH, Battaglia ML. **2021**. Drought stress impacts on plants and different approaches to alleviate its adverse effects. *Plants* **10**: 259.

Soar CJ, Speirs J, Maffei SM, Loveys BR. **2004**. Gradients in stomatal conductance, xylem sap ABA and bulk leaf ABA along canes of *Vitis vinifera* cv. Shiraz: molecular and physiological studies investigating their source. *Functional Plant Biology* **31**: 659–669.

Speirs J, Binney A, Collins M, Edwards E, Loveys B. **2013**. Expression of ABA synthesis and metabolism genes under different irrigation strategies and atmospheric VPDs is associated with stomatal conductance in grapevine (*Vitis vinifera* L. cv Cabernet Sauvignon). *Journal of experimental botany* **64**: 1907–1916.

Sun J, Dong Y, Li C, Shen Y. **2015**. Transcription and enzymatic analysis of beta-glucosidase *VvBG1* in grape berry ripening. *Plant growth regulation* **75**: 67–73.

Tardieu F. **2016**. Too many partners in root–shoot signals. Does hydraulics qualify as the only signal that feeds back over time for reliable stomatal control? *New Phytologist* **212**: 802–804.

Van Ha C, Leyva-González MA, Osakabe Y, Tran UT, Nishiyama R, Watanabe Y, Tanaka M, Seki M, Yamaguchi S, Van Dong N. **2014**. Positive regulatory role of strigolactone in plant responses to drought and salt stress. *Proceedings of the National Academy of Sciences* **111**: 851–856.

Visentin I, Vitali M, Ferrero M, Zhang Y, Ruyter-Spira C, Novák O, Lovisolo C, Schubert A, Cardinale F. 2016. Low levels of strigolactones in roots as a component of the systemic signal of drought stress in tomato. *New Phytologist* **212**: 954–963.

Visentin I, Pagliarani C, Deva E, Caracci A, Turečková V, Novák O, Lovisolo C, Schubert A, Cardinale, F. 2020. A novel strigolactone-miR156 module controls stomatal behaviour during drought recovery. *Plant, cell & environment* **43**: 1613–1624.

Wang Y-T, Chen Z-Y, Jiang Y, Duan B-B, Xi Z-M. **2019**. Involvement of ABA and antioxidant system in brassinosteroid-induced water stress tolerance of grapevine (*Vitis vinifera* L.). *Scientia Horticulturae* **256**: 108596.

Warnock ND, Wilson L, Canet-Perez JV, Fleming T, Fleming CC, Maule AG, Dalzell JJ. **2016**. Exogenous RNA interference exposes contrasting roles for sugar exudation in host-finding by plant pathogens. *International journal for parasitology* **46**: 473–477.

Xiong L, Zhu J-K. **2003**. Regulation of abscisic acid biosynthesis. *Plant physiology* **133**: 29–36.

Xu Z-Y, Kim DH, Hwang I. **2013**. ABA homeostasis and signaling involving multiple subcellular compartments and multiple receptors. *Plant cell reports* **32**: 807–813.

Zhou Y, Minio A, Massonnet M, Solares E, Lv Y, Beridze T, Cantu D, Gaut BS. **2019**. The population genetics of structural variants in grapevine domestication. *Nature plants* **5**: 965–979.